Dynamical properties of type-II superconductors: An experimental study

Y. Brunet* and P. Monceau
Centre de Recherches sur les Très Basses Températures, Centre National de la Recherche Scientifique, Cedex 166, 38042 Grenoble, France

G. Waysand†
Laboratoire de Physique des Solides, Université Paris-Sud, 91405 Orsay, France
(Received 21 February 1974)

We report on surface-resistance measurements of bulk dirty type-II superconductors in the principal orientations between the static magnetic field H, the microwave electric field, and the surface of the sample. When the specimen is in the mixed state, we compare our results with those recently published by Pedersen *et al.* and we emphasize the difficulties inherent in obtaining the conductivity at H_{c2}. When H is parallel to the surface of the sample, the conductivity of the surface sheath is strongly anisotropic. The anisotropy can easily be measured by the ratio of the slopes of the surface resistance in the vicinity of H_{c3} in the two orientations where the microwave electric field is parallel or perpendicular to H. We find, as calculated by Thompson, that this anisotropy is temperature independent within a large range of temperature, and equal to 1 at T_c. These results are in agreement with the formalism of the fluctuations of the order parameter which was first developed by Caroli and Maki. A careful study shows that the anisotropy has a very sharp peak, higher than 1, in the vicinity of T_c, depending on the κ of the sample. The temperature dependence of the anisotropy, as previously reported by Maki and Fischer, can be explained by the bad state of the surface of their samples, or by a misalignment between H and the surface. We also discuss the notion of "nascent vortices" used as an alternative explanation for the anisotropic conductivity of the surface sheath. Finally, we give some results on the angular dependence of the surface impedance.

I. INTRODUCTION

In the last ten years, a great deal of theoretical and experimental work has been done to explain the nonequilibrium properties of type-II superconductors. In particular, one of the most important problems was to understand the resistive behavior of a type-II superconductor when a magnetic field is applied perpendicular to it. Between the two critical fields H_{c1} and H_{c2}, the Abrikosov structure of quantified flux lines or vortices is established, and the transport properties can be described in terms of vortex motion.[1] The first theoretical models treated the mixed state phenomenologically. Bardeen and Stephen[2] generalized the London theory and developed a model in which the current transport flows directly through the normal cores of the vortex lines; this theoretical explanation of dissipation has also been proposed by Rosenblum and Cardona[3] to explain the microwave surface resistance of type-II superconductors. Nozières and Vinen[4] used a hydrodynamic model. For $T=0$, these two models give the same empirical expression for the flux-flow resistivity as obtained by Kim *et al.*,[5] but these models apply only to pure superconductors. Sometime later, Schmid[6] derived a time-dependent Ginsburg-Landau equation (TDGL) and found that near H_{c2}, in the presence of an electric field, the order parameter moves with uniform velocity; he was able to calculate the flux-flow resistivity in the vicinity of the critical temperature T_c. In the study of this problem, Caroli and Maki have made two calculations: the first,[7] (hereafter referred to as CM-I) was the calculation of surface impedance of dirty type-II superconductors within the framework of the linear-response theory. They studied the time dependence of the fluctuations of the order parameter and made the important finding that the microwave conductivity is anisotropic; i.e., it depends on the relative orientation of the microwave field E_ω and the static applied field H. When E_ω is perpendicular to H, the microwave couples the ground state to the excited states of the order parameter, and the conductivity is higher than when $\vec{E}_\omega \parallel \vec{H}$. The second calculation[8] (or CM-II) was the static generalization for all temperatures of the Schmid TDGL equation. But there were some errors in the two calculations which were corrected by Takayama and Ebisawa,[9] as well as by Thompson.[10] In CM-I, some diagrams were forgotten and the conductivity diverged when $\omega \to 0$. With the introduction of these diagrams, it was found that the reactive part of the conductivity was zero, but the dc limit of the absorptive part was not the same as that obtained by the TDGL equations of CM-II. Thompson[10] showed that an "anomalous" term must be taken into account in the expression of the conductivity, so the two results were identical in the dc limit. This "anomalous" term was found by Gor'kov and Eliashberg[11] in their calculation for any order of the response of a superconductor to external fields. One part, the

regular part, was expanded in powers in the order parameter Δ/T_c, and gave the corresponding static expression when $\omega \to 0$; but they found a second or anomalous part, strongly dependent on the ratio of the order parameter to its frequency and momentum, and this gave a finite limit when $\omega \to 0$. It is this term which makes impossible a simple Ginsburg-Landau theory as used by CM-II.[8,12] The same difficulty appeared in the finite frequency conductivity calculation of Fischer *et al.*[13,14] (or FMMM), which was the extension of the static calculation of CM-II. The surface resistance obtained differed by a temperature-dependent numerical factor from that calculated by Thompson.[10]

When the magnetic field is applied parallel to the surface of the superconductor, Saint-James and de Gennes[15] showed that the superconductivity persisted in a layer whose thickness was 1.18 times the coherence length $\xi(t)$ for the critical field $H_{c3} = 1.695\ H_{c2}$. For the sake of generality, let us call Θ the angle between the sample surface and H, and ϕ the angle between the microwave field E_ω and the projection of H onto the surface. Until now, we have been dealing with the *perpendicular* orientation ($\Theta = \pi/2$). In the surface sheath regime (H parallel to the surface), we have two possible orientations: the *longitudinal* orientation with $\Theta = \phi = 0$; and the *transverse* orientation, with $\Theta = 0$ and $\phi = \pi/2$. The surface impedance in the longitudinal orientation was calculated by Maki[16] and by Fischer and Maki,[17] and in the transverse orientation by Maki and Fischer[18]; but due to the same omission as in CM-I, they found a temperature-dependent anisotropy[19] measured by the ratio of the slope in the two orientations of the surface resistance in the vicinity of H_{c3}. Their experimental results also bore this out. By correcting this error, Thompson[20] found that the anisotropy was temperature independent when the corrections to the conductivity in the order of $\omega/\epsilon_0(t)$ were negligible (ω being the microwave frequency and $\epsilon_0(t)$ the intrinsic pair-breaking parameter). We must also point out the calculations of surface resistance using a phenomenological effective conductivity. Rosenblum[21] calculated the effective resistivity of the mixed state as being the sum of the resistivity in the normal regions (vortex cores) and the resistivity in the superconducting regions. In the longitudinal orientation, Rothwarf *et al.*[22] used a two-layer model, the surface sheath being approximated by a uniform-order-parameter layer superposed on the normal bulk. With the values of thickness and the order parameter calculated by Fink and Kessinger,[23] and a Gorter-Casimir[24] temperature dependence for the order parameter, Rothwarf *et al.* found a rather good agreement between the theoretical variation of $R(H_{c2})/R_n$ with the temperature and their experimental results obtained for three different frequencies. The same calculation in the transverse orientation was made by Walton and Rosenblum[25]; but in order to get a realistic conductivity of the superconducting sheath for fields lower than H_{c2}, they postulated the existence at the sample surface of a third layer of vortexlike structures or "nascent vortices."[26] We shall discuss the existence of this structure in Sec. V.

Experimental results[27] exhibited a very sharp minimum for $\Theta = 0$ in the surface-resistance measurements. Kulik[28] showed that, for an inclined magnetic field ($\Theta \neq 0$), the surface sheath had a vortex structure similar to that found by Abrikosov. Taking into account these tilted vortices, Maki[29,30] calculated the surface impedance as a function of Θ in the two cases $\phi = 0$ and $\phi = \pi/2$.

We report surface-resistance measurements on bulk type-II superconductors whose thickness d is much greater than the normal microwave penetration depth δ_0.[31] Our results on pseudobulk samples with $10\xi(t) \ll d \ll \delta_0$ were published earlier.[32] In Sec. II we review the theoretical expressions for the surface resistance from the more general response functions of a superconductor to a microwave field. In Sec. III we describe the experimental apparatus and the samples used. In Sec. IV we present the experimental data. We first discuss the results in the mixed state. We find that, at low temperature, the anisotropy in the surface sheath regime is temperature independent; we can explain that the dependence on temperature, as found earlier by Maki and Fischer,[18] is due to a misalignment of H and the surface of the sample; the influence of a badly polished surface will also be studied. The anisotropy becomes equal to 1 at T_c when the fluctuations of the order parameter cannot be excited by the microwave field. A detailed study will show that the anisotropy has a maximum higher than 1 in the immediate vicinity of T_c.

II. THEORY

We assume that the superconductor occupies half the space $z \geq 0$, and that the surface of the sample lies in the xy plane. The microwave is emitted from $z \to -\infty$. In the perpendicular orientation, the static magnetic field is applied along the z axis. When H is parallel to the surface along the x axis, E_ω is along the x axis in the longitudinal orientation, and along the y axis in the transverse one. H may be rotated in the xz plane, and has an angle Θ with the surface as shown in Fig. 1.

A. Response functions to the microwave field

In the general case, the relationship between the microwave current and the microwave vector potential A_ω (with the time dependence of the form $e^{-i\omega t}$) is expressed by the formula

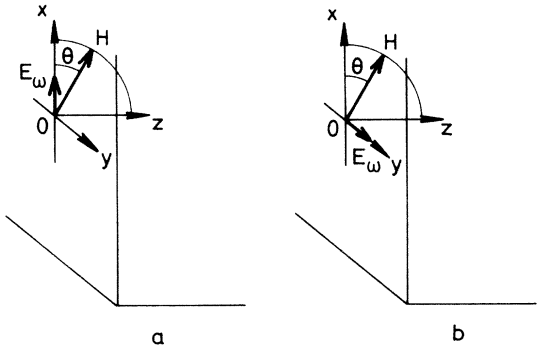

FIG. 1. Two geometrical configurations when the static magnetic field is tilted away from the surface of the sample which lies in the xy plane. ϕ is the angle between the microwave field E_ω and the projection of H on the surface. (a) $\phi = 0$ ($\Theta = 0$ corresponds to the longitudinal orientation; (b) $\phi = \frac{1}{2}\pi$ ($\theta = 0$ corresponds to the transverse orientation).

$$j_\omega = -QA_\omega ,$$

where Q is the response function. j_ω is the sum of two parts: $j_\omega = j_n + j'$; $j_n = -Q_n A_\omega = -i\omega\sigma_n A_\omega$ is the current in the normal state, σ_n being the normal-state conductivity of the superconductor, and $j' = -Q'A_\omega$ is the small perturbation due to the superconductivity which is proportional to the mean-square average of the order parameter $\langle|\Delta|^2\rangle$. Q' has been calculated by several authors;

$$Q' = Q'_{\text{stat}} + Q'_{\text{CM}} + Q'_T .$$

Q'_{stat} is the response function without the assumption of a possible spatial variation of the order parameter. This is the response in the longitudinal orientation. Q'_{stat} was first calculated by Maki, [16] and its expression is given in the Appendix. In the limit $\omega \ll \pi T_c$

$$Q'_{\text{stat}} = (\sigma_n|\Delta|^2/\pi T)\,\Psi^{(1)}(\tfrac{1}{2}+\rho_0)\,\tilde{Q}'_{\text{stat}} ,$$

with [Eq. (A1)]

$$\tilde{Q}'_{\text{stat}} = 1 + \frac{1}{2}\frac{-i\omega}{-i\omega+\epsilon_0} - \frac{i\omega}{8\pi T}\left(3 + \frac{-i\omega}{-i\omega+\epsilon_0}\right)\frac{\Psi^{(2)}(\frac{1}{2}+\rho_0)}{\Psi^{(1)}(\frac{1}{2}+\rho_0)} ,$$

$$\rho_0 = \epsilon_0/4\pi T, \quad \epsilon_0 = 2eDH_{c2} ,$$

$$\ln t = \Psi(\tfrac{1}{2}) - \Psi(\tfrac{1}{2}+\rho_0) .$$

e is the magnitude of the electronic charge, $D = \frac{1}{3}v_F l$ is the diffusion constant, Ψ is the digamma function, and $\Psi^{(1)}$ and $\Psi^{(2)}$ are the first and second derivatives of Ψ (we choose units $\hbar = c = k = 1$).

Q'_{CM} is the contribution calculated by CM-I, [7] taking into account the modes associated with the fluctuations of the order parameter induced by the microwave field. These modes are intimately connected to the spatial variation of the order parameter, and their contribution exists only if $\vec{E}_\omega \perp \vec{H}$. The order parameter deviates from its equilibrium value or from its lowest eigenmode $|0\rangle$. The microwave induces higher diffusive modes $|n\rangle$ which decay exponentially with time according to $e^{-\epsilon_{n0}t}$; the damping coefficient ϵ_{n0} is equal to $\epsilon_n - \epsilon_0$, where ϵ_n is the eigenvalue of the nth excited state. As has been pointed out in Sec. I, CM-I, in their calculation, forgot some very important diagrams in the perpendicular orientation and Thompson[10] found a correcting term Q_T. The more general expression of Q'_{CM} [Eq. (31) of Ref. 7] and of Q_T [Eq. (10) of Ref. 10] is given in the Appendix.

Let us call $Q'_{\text{CM}} + Q'_T = Q'_{\text{fluct}}$. In the low-frequency limit $\omega \ll \pi T_c$, Q'_{fluct} can be expressed by

$$Q'_{\text{fluct}} = (\sigma_n|\Delta|^2/\pi T)\,\Psi^{(1)}(\tfrac{1}{2}+\rho_0)\,\tilde{Q}'_{\text{fluct}} ,$$

with [Eq. (A2)]

$$\tilde{Q}'_{\text{fluct}} = -\sum_n x_n\left[\frac{4}{\epsilon_{n0}-i\omega}\left(1 - \frac{i\omega}{4\pi T}\frac{\Psi^{(2)}(\frac{1}{2}+\rho_0)}{\Psi^{(1)}(\frac{1}{2}+\rho_0)}\right)\right] ,$$

where $x_n = D|\langle n|2e\vec{A}|0\rangle|^2$ is the square of the matrix element of the vector potential between the nth excited state and the ground state. Let us now examine the different orientations:

1. Mixed state ($\phi = \pi/2$)

The ground state $\epsilon_0 = 2eDH_{c2}$ is the Abrikosov solution, and the eigenvalues are those of the harmonic oscillator $\epsilon_n = (2n+1)\epsilon_0$. The $n = 1$ mode corresponds to a collective oscillation, at the frequency ω, of the vortex lattice along $\vec{E}_\omega \times \vec{H}$; the only nonvanishing matrix element is $x_1 = eDH_{c2}$.

2. Surface sheath regime ($\Theta = 0$)

The ground state $\epsilon_0 = 0.59(2eH_{c3})$ is the Saint-James–de Gennes[15] solution. The excited states of the surface sheath were calculated by Fink, [33] who gave their eigenvalues as a function of the square of the distance between the nucleation site and the surface. Near H_{c3} the microwave can only excite states with the same nucleation site as the ground state. The energies of these states are $5.6\epsilon_0$ for $n = 1$ and $11.05\epsilon_0$ for $n = 2$. In the longitudinal orientation, the matrix elements are zero and the fluctuations are not excited. In the transverse orientation, the matrix element $D|\langle 1|2eHz|0\rangle|^2 = 0.59eDH_{c3}$. As the contribution of the excited states decreases as $e^{-\epsilon_{n0}t}$, the first excited state almost gives the full contribution (within 7%). Physically, the fluctuations are induced by the coupling between the microwave current and the screening current in the surface sheath. The $n = 1$ mode is along $\vec{E}_\omega \times \vec{H}$, and corresponds to an oscillation (at the frequency ω) of the surface sheath itself perpendicular to the surface of the sample.

3. Tilted magnetic field

In the tilted case (H in the xz plane) the order parameter for the equilibrium state and the excited

TABLE I. Ground-state energy; damping coefficients $\epsilon_{n0}=\epsilon_n-\epsilon_0$, where ϵ_n is the eigenvalue for the nth excited state; the square of matrix elements $x_n=D\langle n|2eA|0\rangle|^2$ of the vector potential between the nth excited state and the ground state; and anisotropy for (a) the mixed state, (b) the surface sheath regime in the longitudinal ($\phi=0$) and transverse ($\phi=\frac{1}{2}\pi$) orientations, and (c) when the magnetic field is tilted away from the surface of the sample.

		Mixed state	Surface sheath		Inclined magnetic field	
			$\phi=0$	$\phi=\frac{1}{2}\pi$	$\phi=0$	$\phi=\frac{1}{2}\pi$
Ground-state energy		$\epsilon_0(\rightarrow H_{c2})$	$0.59\epsilon_0(\rightarrow H_{c3})$		$\alpha(\Theta)\epsilon_0(\rightarrow H_{c3}(\theta))$	
Damping coefficients	$\epsilon_1-\epsilon_0$	$2\epsilon_0$	$4.6\epsilon_0$		$2\epsilon_0\sin\theta$	
	$\epsilon_2-\epsilon_0$	$4\epsilon_0$	$10.05\epsilon_0$		$2.7\epsilon_0\cos\theta$	
	...					
Matrix elements	x_1	$\frac{1}{2}\epsilon_0$	0	$\frac{1}{2}\epsilon_0$	$2\epsilon_0\sin\theta$	$0.319\ (2\epsilon_0\sin\theta)$
	x_2	0	0	...	0	$1.18\epsilon_0\cos\theta$
	...					
Anisotropy A		0	0.586		...	

states has to be determined. It is much more complicated, because the differential equation for $\Delta(x, z)$ is not separable into operators depending only on x or z. Maki[30] constructed the ground-state and excited-state wave functions in terms of the product space $(\phi_0, \phi_1)\times(\Psi_0, \Psi_1)$, where ϕ_0 and ϕ_1 are the ground-state and the first-excited-state functions for the Abrikosov state, and Ψ_0 and Ψ_1 are those for the surface sheath. The ground state is a solution where, as Kulik[28] showed, the surface sheath has a vortex structure similar to the mixed state. (Because in his calculation Kulik used a linear Ginsburg-Landau equation, he could neither calculate nor minimize the free energy and subsequently was unable to obtain information about the geometrical structure of the vortex lattice in the superconducting sheath.) The lowest eigenvalue $\alpha(\Theta)$ determines the critical field $H_{c3}(\Theta)$ as

$$\epsilon_0=\alpha(\Theta)[2eDH_{c3}(\Theta)]$$

and

$$H_{c3}(\Theta)/H_{c2}=\{2\sin\Theta+1.95\cos\Theta-[(\sin\Theta+1.36\cos\Theta)^2+0.59\sin\Theta\cos\Theta]^{1/2}\}^{-1}\ .$$

This expression is only valid for small Θ and gives $(1/H_{c3})(dH_{c3}/d\Theta)|_{\Theta=0}=-1.33|\Theta|$, whereas the Saint-James[34] result is $-1.35|\Theta|$. The eigenvalues and matrix elements are given in Ref. 30 in the two orientations $\Theta\neq0$, $\phi=0$ and $\Theta\neq0$, $\phi=\pi/2$. All coefficients are summarized in Table I.

B. Surface impedance calculations

Our calculations closely follow those of Thompson,[20] who has made a careful calculation of the surface impedance Z. Using the standard definition of

$$Z=R-iX=4\pi\frac{E_\omega(0)}{H_\omega(0)}$$

$$=4\pi i\omega A_\omega(z)\Big/\frac{\partial}{\partial z}A_\omega(z)|_{z=0}\ ,$$

[$E_\omega(0)$ and $H_\omega(0)$ being the electric and magnetic components, respectively, of the microwave field at $z=0$], and the differential equation for the vector potential inside the superconductor

$$-\frac{\partial^2A}{\partial z^2}=|4\pi j_n(z)+j'(z)|\ ,$$

Thompson calculated the general expression of Z

$$Z=-4\pi i\omega\delta\frac{A_0+2\pi\delta\int_0^\infty e^{-z/\delta}j'(z)\,dz}{A_0-2\pi\delta\int_0^\infty e^{-z/\delta}j'(z)\,dz}\ . \qquad (1)$$

δ is the complex penetration depth $\delta=(-4\pi i\omega\sigma_n)^{-1/2}=\frac{1}{2}(1+i)\delta_0$ and $\delta_0=(2\pi\omega\sigma_n)^{-1/2}$ is the normal-state classical skin depth. j' is calculated in the presence of the normal potential $A_0e^{-z/\delta}$; as in the case of our experiments on dirty superconductors, Q' is local, and $j'(z)=-A_0Q'(z)e^{-z/\delta}$. We can develop the expression (1) and

$$Z=-4\pi i\omega\delta[1-4\pi\delta\int_0^\infty e^{-2z/\delta}Q'(z)\,dz]\ . \qquad (2)$$

Let us look at the different orientations.

1. Mixed state

In this orientation, Q' is constant and we find

$$Z=-\frac{4\pi i\omega}{(4\pi Q_n)^{1/2}}\left(1-\frac{Q'}{2Q_n}\right).$$

The surface resistance is equal to

$$R=R_n\left(1-\frac{\mathrm{Im}Q'-\mathrm{Re}Q'}{2\omega\sigma_n}\right), \tag{3}$$

where R_n is the surface resistance of the normal state. With the value of Q' taken from the Appendix, the coefficients from Table I, and Eq. (A3) of $\langle|\Delta|^2\rangle$ in the mixed state, Eq. (3) can be expressed as

$$R=R_n\left(1-\frac{2\kappa_1^2(0)L_D(t)}{1.16[2\kappa_2^2(t)-1]+n}[H-H_{c2}(t)]f_1(t,\omega)\right) \tag{4}$$

with

$$L_D(t)=2+\rho_0\frac{\Psi^{(2)}(\frac{1}{2}+\rho_0)}{\Psi^{(1)}(\frac{1}{2}+\rho_0)}.$$

κ_1 and κ_2 are the generalized Ginsburg-Landau parameters; n is the demagnetization coefficient; $L_D(t)$ equals one at $T=0$ and two at $T=T_c$. In the static limit $\omega\ll\pi(T_c-T)\sim\epsilon_0(t)$, $\mathrm{Re}Q'/\omega\equiv 0$ and the static conductivity is given by the $\mathrm{Im}Q'/\omega$ term. $f_1(t,\omega)$ gives the frequency dependence of R/R_n as a function of $\omega/\pi(T_c-T)$ and ω/T_c. Experimentally, we measure the slope of the surface resistance near H_{c2} and the results are presented in terms of normalized slopes at H_{c2}

$$s_1=\frac{H_{c2}}{R_n}\frac{\partial R}{\partial H}\bigg|_{H=H_{c2}}. \tag{5}$$

The temperature variation of s_1 for different values of $\omega/\pi T_c$ is shown by Pedersen *et al.*[35] The only difference between Eq. (4) and the expression obtained by CM-II or FMMM[13] is the factor $L_D(t)$. However, we must recall the zone of validity of these two theories. As pointed out by Thompson,[10] the CM-II result consists only of regular terms and the zone of validity is that of the Ginsburg-Landau equations; i.e., $\Delta\ll\pi T_c$ or, expressed in magnetic field, $1-H/H_{c2}(t)\ll 1$. On the other hand, the Thompson term includes an anomalous term and the zone of validity is reduced to $\Delta\ll\epsilon_0(t)$, or $1-H/H_{c2}(t)\ll 1-t$. Finally, Takayama and Maki[36] have made calculations of the conductivity in this region, taking into account the effect of higher-order corrections of the order parameter.

2. Surface sheath regime

Q' is no longer constant, but decreases exponentially inside the superconductor. If $|\Delta(z)|^2$ is approximated to a Gaussian variation $|\Delta(z)|^2=|\Delta(0)|^2e^{-z^2/2\xi^2(t)}$, we can write Eq. (2) as

$$Z=-4\pi i\omega\delta\left(1-\frac{4\pi\delta\sigma_n}{\pi T}\Psi^{(1)}\left(\frac{1}{2}+\rho_0\right)\tilde{Q}'(\omega)\times\int_0^\infty e^{-2z/\delta}e^{-z^2/2\xi^2(t)}\,dz\right). \tag{6}$$

Therefore we must consider two cases in which $|\Delta|^2$ becomes negligible for distances either greater or smaller than $\xi(t)$.

a. $\xi(t)\ll\mathrm{Re}\delta$. This condition requires[20]

$$\omega/\pi(T_c-T)\ll 2\kappa^2. \tag{7}$$

The temperature range in which Eq. (7) is not satisfied decreases as κ increases. Eq. (6) can easily be integrated. With the expression for $|\Delta|^2$ obtained by Maki[37] and given in Eq. (A4)

$$Z=R_n(1-i)\left(1-\frac{(1+i)\delta_0}{2\xi(t)}\frac{H_{c3}-H}{H_{c3}}\times\frac{1}{2\kappa_2^2(t)-0.328}(\mathrm{Re}\tilde{Q}'+i\,\mathrm{Im}\tilde{Q}')\right).$$

The real part of Z is

$$R=R_n\left(1-\alpha\,\mathrm{Re}\tilde{Q}'\frac{H_{c3}(t)-H}{H_{c3}(t)}\right) \tag{8}$$

with

$$\alpha=\frac{\delta_0}{\xi(t)}\frac{1}{2\kappa_2^2(t)-0.328}.$$

In the low-frequency limit $\omega\ll\pi T_c$, according to Eqs. (A1) and (A2) in the longitudinal and transverse orientations,

$$\mathrm{Re}\tilde{Q}_l'=1+\tfrac{1}{2}\omega^2/(\omega^2+\epsilon_0^2), \tag{9}$$

$$\mathrm{Re}\tilde{Q}_{tr}'=1+\frac{1}{2}\frac{\omega^2}{\omega^2+\epsilon_0^2}-\frac{2\times 4.6\epsilon_0^2}{(4.6\epsilon_0)^2+\omega^2}\times\left(1-\frac{\omega^2\rho_0}{4.6\epsilon_0^2}\frac{\Psi^{(2)}(\frac{1}{2}+\rho_0)}{\Psi^{(1)}(\frac{1}{2}+\rho_0)}\right). \tag{10}$$

The calculation depends only on regular terms and the zone of validity as expressed in magnetic field is $1-H/H_{c3}(t)\ll 1$.

b. $\xi(t)\gg\mathrm{Re}\delta$. We have to calculate the integral in Eq. (6). This integral is complex and Maki[38] made some approximations; this leads to the following result:

$$Z=R_n(1-i)[1-\tfrac{1}{2}(1+i)\hat{\alpha}(1+iP)(\mathrm{Re}\tilde{Q}'+i\,\mathrm{Im}\tilde{Q}')], \tag{11}$$

where

$$\hat{\alpha}=\left\{\left[1+\frac{2}{\sqrt{\pi}}\left(\frac{\xi}{\delta_0}\right)\right]\Big/\left[\left(1+\frac{2}{\sqrt{\pi}}\frac{\xi}{\delta_0}\right)^2+\frac{4}{\pi}\left(\frac{\xi}{\delta_0}\right)^2\right]\right\}\alpha$$

and

$$P=\frac{2}{\sqrt{\pi}}\frac{\xi}{\delta_0}\frac{1}{1+(2/\sqrt{\pi})(\xi/\delta_0)}.$$

The real part of Eq. (11) gives

$$R = R_n\left(1 - \hat{\alpha}(\mathrm{Re}\tilde{Q}' - P\mathrm{Im}\tilde{Q}')\frac{H - H_{c3}(t)}{H_{c3}(t)}\right) . \quad (12)$$

If $\xi(t) \ll \mathrm{Re}\delta$, Eq. (8) is again the result; if $\xi(t) \gg \mathrm{Re}\delta$, then $P = 1$, and we are in a situation where Q' is constant over the skin depth, as in the mixed state. We experimentally measure the slopes of the surface resistance near H_{c3}, and we can define the normalized slopes:

$$s_{l,\mathrm{tr}} = \frac{H}{R_n}\frac{\partial R}{\partial H}\bigg|_{H=H_{c3}} = \hat{\alpha} f_{l,\mathrm{tr}}(t, \omega) . \quad (13)$$

In Fig. 2 we have drawn the theoretical variations of $f_{l,\mathrm{tr}}(t, \omega)$ for a $Pb_{97}In_3$ alloy at 9.5 GHz and $T_c = 7\,\mathrm{K}$ ($\omega/T_c = 0.064$), emphasizing the region near T_c.

3. *Inclined magnetic field*

Although it is possible to have the general expressions of Z as a function of t, ω, Θ from the general expression of $\tilde{Q}'$, we shall study the surface impedance within the limit of $\omega \ll \epsilon_0(t)$. We only have the contribution of $\mathrm{Re}\tilde{Q}'$. Z is equal to

$$Z = R_n\left[1 - i - \alpha(H, \Theta)\frac{H_{c3}(\Theta) - H}{H_{c3}(\Theta)} \times \left(1 - \frac{x_1^2}{\epsilon_{10} - i\omega} - \frac{x_2^2}{\epsilon_{20} - i\omega}\right)\right] ,$$

where $\alpha(H, \Theta)$ is the generalization of α;

$$\alpha(H, \Theta) = \frac{\delta_0}{\xi^2(t)}\left(\frac{2\pi}{1.18eH\cos\Theta}\right)^{1/2} \times \frac{1}{1.16(2\kappa_2^2(t) - 0.334\cos\Theta - \sin\Theta)} ;$$

and x_1, x_2, ϵ_{10}, ϵ_{20} are in Table I. In the longitudinal orientation,

$$R = R_n\left(1 - \alpha(H, \Theta)\frac{H_{c3}(\Theta) - H}{H_{c3}(\Theta)}\frac{\tilde{\omega}^2}{1 + \tilde{\omega}^2}\right) , \quad (14)$$

and in the transverse orientation,

$$R = R_n\left[1 - \alpha(H, \Theta)\frac{H_{c3}(\Theta) - H}{H_{c3}(\Theta)}\left(\frac{0.319\tilde{\omega}^2}{1 + \tilde{\omega}^2} + 0.247\right)\right] , \quad (15)$$

with

$$\tilde{\omega} = \frac{\omega}{4eDH\sin\Theta} . \quad (16)$$

When $\Theta \to 0$ and $\omega \ll \epsilon_0(t)$, we again find Eq. (8). The surface resistance has a sharp peak for $\Theta = 0$ and the width of this peak is of the order of $\omega/4eDH$; for the frequency of our measurements, which is 2.4 GHz, and for $H \sim 3000$ Oe, Θ is equal to 0.3°. It is a clear indication of a very good alignment which is necessary between H and the surface of the sample.

C. Anisotropy

The anisotropy is measured by the ratio of the slopes of R/R_n in the longitudinal and transverse orientations. In the static limit $\omega \ll \epsilon_0(t)$

$$A = \mathrm{Re}Q'_{\mathrm{tr}}/\mathrm{Re}Q'_l .$$

In the mixed state $\mathrm{Re}Q'_{\mathrm{tr}} \equiv 0$ and $A = 0$. The anisotropy is complete: there is no screening current in the mixed state. In the surface sheath regime, within the static limit, $A = 1 - 2/4.6 = 0.57$. Summing over all the excited states, Thompson[20] found $A = 0.586$. Maki and Fischer,[18] in their incorrect calculation, found a temperature-dependent anisotropy

$$A = 1 - \frac{2[\Psi(\frac{1}{2} + 5.62\rho_0) - \Psi(\frac{1}{2} + \rho_0)]}{(4.62)^2\rho_0\Psi^{(1)}(\frac{1}{2} + \rho_0)} , \quad (17)$$

where this value was 0.57 at T_c and 0.84 at $T = 0$. After Eqs. (9) and (10) we see that, near T_c, $\mathrm{Re}Q'_{\mathrm{tr}} \to \mathrm{Re}Q'_l$ and then $A \to 1$. At T_c, when $\omega > \epsilon_0(t)$, there is no more anisotropy because the fluctuations of the order parameter cannot follow the exciting field. Physically, at T_c the order parameter Δ is homogeneous over the skin depth, and the fluctuations being related to the spatial variation of Δ become irrelevant. In Fig. 2 it is possible to see that the two curves $f_l(t, \omega)$ and $f_{\mathrm{tr}}(t, \omega)$ intercept each other near T_c. There is a region where the anisotropy is higher than 1. According to Eq. (12), the general expression of the anisotropy can be expressed as

$$A = \frac{\mathrm{Re}\tilde{Q}'_{\mathrm{tr}} - P\mathrm{Im}\tilde{Q}'_{\mathrm{tr}}}{\mathrm{Re}\tilde{Q}'_l - P\mathrm{Im}\tilde{Q}'_l} . \quad (18)$$

In Fig. 2 we have plotted the theoretical variation of A near T_c as a function of t at three different values of $\omega/T_c = 0.016$, 0.07, and 0.15 corresponding to a critical temperature of 7 K to frequencies of 2.4, 9.5, and 23 GHz.

When the magnetic field is tilted away from the surface, the anisotropy is defined according to Eqs. (14) and (15). In the static case,

$$A = 0.565 + 0.247\tilde{\omega}^2 ; \quad (19)$$

we can plot A as a function of $\omega^{-1} = 4eDH_{c3}(\sin\Theta)/\omega = (3.38\epsilon_0/\omega)\sin\Theta$. Near T_c, ϵ_0 is proportional to $(1 - t)$. In Fig. 3, A is plotted as a function of t for two different values of Θ, 0.5° and 1°.

III. EXPERIMENTAL TECHNIQUE AND SAMPLES

The surface impedance is measured by a resonance technique. The specimen forms part or all of a resonator. The inverse of the quality factor Q is proportional to the surface resistance, and the shift of the resonance frequency is proportional to the surface reactance. For our measurements at 2.4 GHz, we use a technique similar to the one used by Pippard[39] and Waldram.[40] The resonator is a

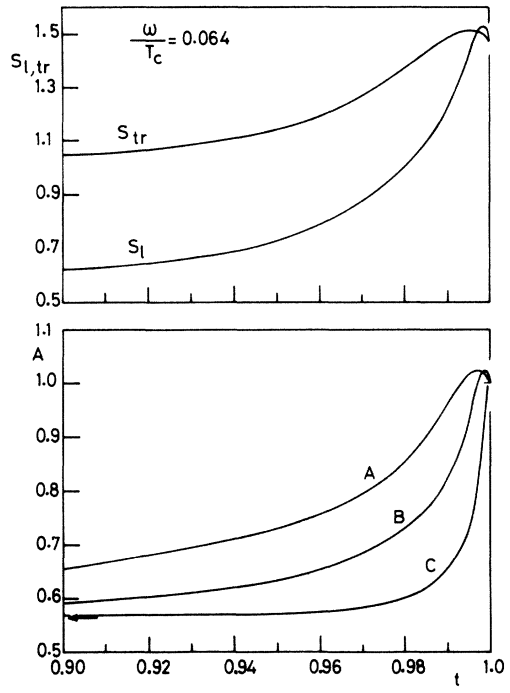

FIG. 2. Upper graph shows the temperature variation of the frequency-dependent part of the theoretical expressions of the slopes $s_{l,tr} = (H/R_n)(\partial R/\partial H)\,|_{H=H_{c3}}$ in the longitudinal and in the transverse orientation for $\omega/T_c = 0.064$. The lower part is the anisotropy (or the ratio between s_{tr} and s_l) near T_c for different values of ω/T_c: A, 0.15; B, 0.07; and C, 0.016. In the extreme vicinity of T_c the anisotropy is higher than 1 and equal to 1 at $T = T_c$. The arrow indicates the static limit value of A.

U-shaped strip, magnetically coupled to a transmission line formed by two coaxial lines connected by a small coupling loop. In order to have the full power transmitted without resonance at our disposition, we must compensate the inductance of the coupling loop by a reactive element located at its center. This element is made of a short coaxial transmission line around which a quartz tube can slide. The over-all dimensions of the **U** are 28×7×5 mm, and the spacing between the inner faces of the **U** is 3 mm. In previous experiments[41,42] the **U** was made entirely of the superconductor whose surface impedance we wished to measure. We had an electromechanical feedback system to measure the ratio of the signals from two square-law detectors D_1 and D_2 for each value of the magnetic field applied; the first, D_1, measured part of the power delivered by the generator and the other, D_2, measured the power transmitted. The minimum value at the resonance was obtained by slowly sweeping the frequency across the resonance. The equivalent circuit was studied earlier.[43] It was then shown how the surface resistance normalized to the normal state was derived from the measurements of the minimum of the power transmitted at the resonance. In the present experiments, we have improved the technique to obtain continuous recordings of the surface resistance as a function of the magnetic field. First, we have an automatic regulation (by a pin-diode circuit) of the power delivered by the generator. This regulator is controlled by the dc voltage measured by the detector D_1. Second, the klystron frequency is locked to the cavity resonance frequency by a stabilization system. On an x-y recorder, the y axis is driven by the dc voltage across D_2, and the x axis by a voltage proportional to the applied magnetic field. The **U** is a copper or aluminum strip, and the samples (5×5×0.3 mm) are glued inside the **U** on the flat surfaces. The variation of the minimum at the resonance between the normal and superconducting state is only a few percent of the superconducting-state value; for each experiment we make sure that the direct voltage recorded, as measured by D_2 as a function of the magnetic field, gives the true variation of the surface resistance.[43] The resonator is inside a double calorimeter and the experiments can be carried out between 1.2 and 20 K. The temperature is regulated electronically and the temperature stabilization is better than 10^{-4} K. The magnetic field is produced by an 8-kG electromagnet, which can be rotated so that H can be either perpendicular or parallel to the sample surface (transverse orientation); the angular resolution is 0.2°. To make measurements in the longitudinal orientation, we use a superconducting magnet ($H/I = 485$ Oe/A). In Sec. II, the extreme importance of a good alignment between H and the surface of the sample has been shown; that is why, in this orientation, nitrogen-cooled Helmotz coils ($H/I = 19$ Oe/A) were built; these give a small perpendicular field and correct a possible misalignment. Experimentally, in the transverse orientation, we apply a magnetic field $\sim H_{c2}$, and we rotate the electromagnet to get a minimum in the surface resistance.[42] In the longitudinal orientation, we apply a current in the superconducting magnet producing a field $\sim H_{c2}$ and

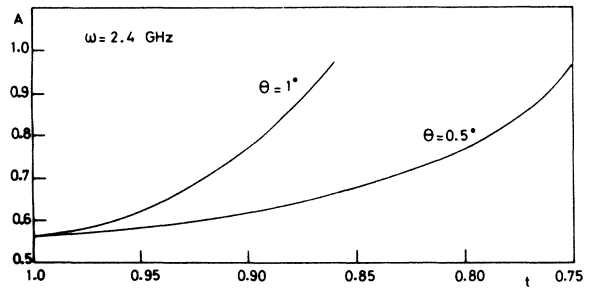

FIG. 3. Anisotropy as a function of t for two different values of the angle between H and the surface of the sample at 2.4 GHz according to Eq. (16).

TABLE II. Sample characteristics.

Alloy	ρ_n ($\mu\Omega$ cm)	D (cm^2 sec^{-1})	$T_c(\kappa)$	l/ξ_0	κ [a]
$Pb_{50}In_{50}$	21.3	6.17	6.48	0.056	7.35
$Pb_{90}In_{10}$	7.95	14.2	7.02	0.152	2.95
$Pb_{97}In_3$	2.37	36.5	7.12	0.51	1.15
$Nb_{80}Mo_{20}$	6.8	10.5	4.3	0.127	4.2

[a] κ is calculated from resistivity and specific heat.

we determine which amplitude of the current in the Helmotz coils gives the minimum in surface resistance. We can thus find the ratio between the two currents, and we use an automatic circuit in the power supply to keep this ratio constant when the current in the superconducting magnet is either increased or decreased.

Pb-In samples and one $Nb_{80}Mo_{20}$ sample were used. We have used Pb-In alloys previously[41, 42] and their characteristics can be found in Table II. The samples were carefully polished using Wormer and Wormer's[44] reagent. Lead-indium alloys are strong coupling superconductors and, among other properties, the ratio of their gap to their critical temperature $2\Delta(0)/kT_c$ is ~4.3[45] compared to the theoretical BCS weak coupling value 3.5.[46] French and Lowell[47] showed that, in the Nb-Mo system, the coupling becomes weaker when the MO content is increased, and that the $Nb_{80}Mo_{20}$ alloy could be considered a weak coupling superconductor. A similar sample, which we have produced in an induction furnace, has a critical temperature and resistivity comparable to those obtained by French and Lowell. It was mechanically polished and electropolished. To evaluate l/ξ_0, we took $\rho l = 3.7\times10^{-12}$ Ω cm^2[48] and $\xi_0 = 430$ Å,[49] as for niobium.

Typical experimental curves are shown in Fig. 4.

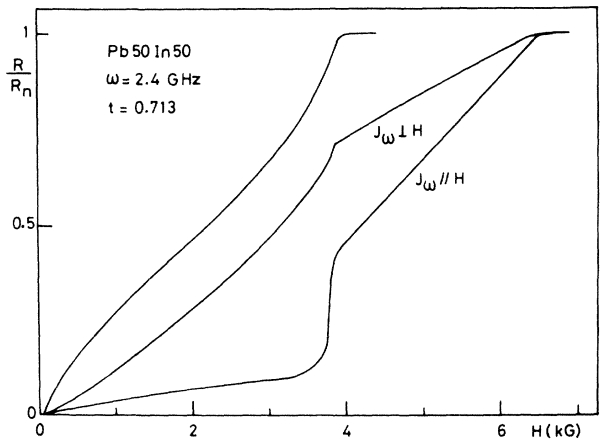

FIG. 4. Experimental surface resistance normalized to the normal state as a function of the magnetic field in the perpendicular, transverse, and longitudinal orientations.

For well-polished and well-annealed samples, such as the lead-based alloys, the R/R_n curves are reversible and no hysteresis can be observed.

IV. EXPERIMENTAL DATA AND DISCUSSION

A. Mixed state

In Sec. II, we have seen that the Thompson[10] and FMMM[13] theories are valid for two different ranges of magnetic fields. It is very difficult to experimentally measure the slope of R/R_n at H_{c2} because of rounding due to inhomogeneities in the sample. When the slope is not taken exactly at $H = H_{c2}$, but in a region where R/R_n has a linear variation with H, a good agreement is obtained with FMMM.[13] Pedersen *et al.*[35] have made direct measurements of the slope $\partial R/\partial H$ as a function of H. Their curves did not have a sharp transition at H_{c2}, but the slope showed a slight increase before showing a gradual decrease down to the zero value (part AB in the insert of Fig. 5); H_{c2} was determined in the center of this decreasing part. To get the $\partial R/\partial H$ value at H_{c2} (point S), they extrapolated the linear increasing

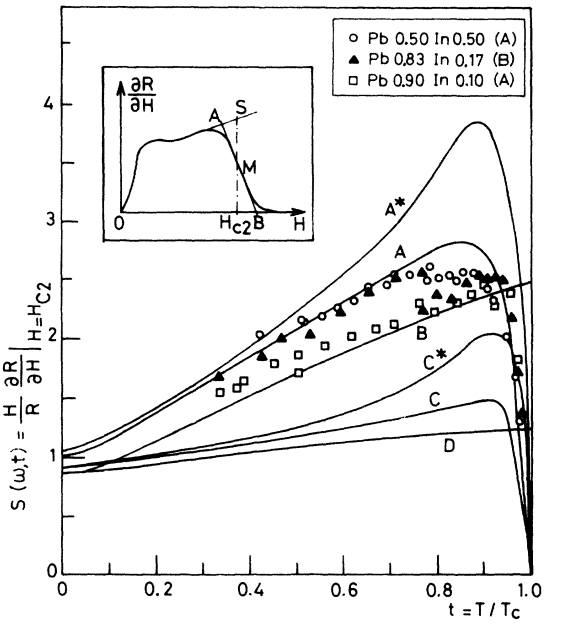

FIG. 5. Results of Pedersen *et al.* obtained with a derivative technique for Pb-In alloys. The curves A and B for $\omega = 31.4$ GHz and $\omega = 0$ according to the Thompson[10] theory, and the curves C and D for the same frequencies according to the theory of Fischer *et al.*,[13] were obtained with the theoretical variation of $\kappa_2(t)$ as calculated by Caroli *et al.* We show the theoretical variations A^* and C^* for the two theories at 31.4 GHz using the experimental temperature variation of $\kappa_2(t)$. The insert shows the extrapolation made by Pedersen *et al.* to obtain the slope at H_{c_2} and circumvent the rounding in the curves due to inhomogeneous samples.

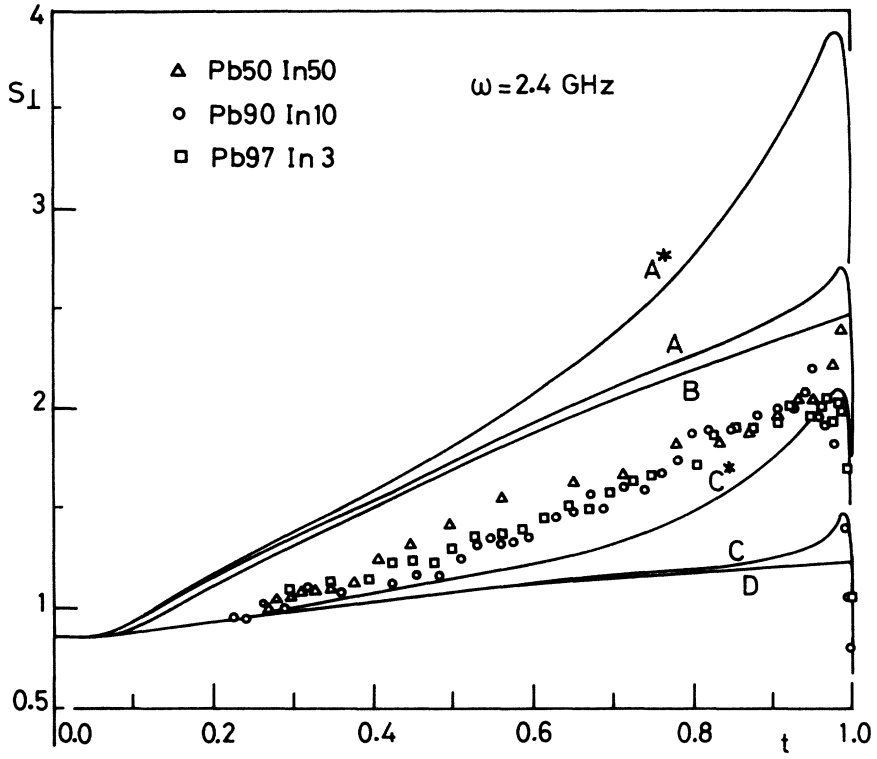

FIG. 6. Our results on lead-indium alloys at 2.4 GHz with the same theoretical curves as in Fig. 5, calculated for the frequency of our measurements.

slope up to the $H = H_{c2}$ line. Following Eqs. (4) and (5),

$$s_\perp = \frac{2\kappa_1^2(0)}{1.16[2\kappa_2^2(t)-1]+n} L_D(t) f_\perp(\omega, t) \ . \qquad (20)$$

In the case of high κ_2 values, and using the relation $\kappa_1(0) = \kappa_2(0)$, which is valid only for weak coupling dirty superconductors, Eq. (20) can be written

$$s_\perp \cong 0.862[\kappa_2(0)/\kappa_2(t)]^2 L_D(t) f_\perp(\omega, t) \ . \qquad (21)$$

In order to compare the experimental $s_\perp$ measurements with the theoretical calculations, we need to know the temperature variation of κ_2. This variation was obtained by Caroli *et al.*[50] for extremely dirty superconductors. Eilenberger[51] calculated the variation of $\kappa_2(t)/\kappa_2(1)$ and $\kappa_1(t)/\kappa_1(0)$ for different l/ξ_0 ratios based on the following two principal assumptions: (i) a spherical Fermi surface and (ii) a weak electron-phonon interaction; the temperature variation of κ_2 became more important as l/ξ_0 increased. Usadel[52] showed that the strong coupling correction to the variation of κ_2 with t was very small. Pedersen *et al.* measured $s_\perp$ for two different systems: Nb-Ta and Pb-In alloys. $\kappa_2(t)$ for Nb-Ta alloys was determined by Ikushima and Mizusaki.[53] For concentrations higher than 19.7 at.%, they found a good agreement with the result of Caroli *et al.*; i.e. $\kappa_2(0)/\kappa_2(1) = 1.2$. Consequently, the use of this theoretical variation of $\kappa_2(t)$ in Eq. (21) (by Pedersen *et al.*[35] in their Fig. 8) was appropriate. Pedersen *et al.* found that their experimental $s_\perp$ measurements were situated between the Thompson and FMMM theoretical curves. It is proved experimentally[41,54] that, for Pb-In alloys, κ_2 has a much stronger temperature dependence than expected, according to the theory; for example, $\kappa_2(0)/\kappa_2(1) \cong 1.4$ or 1.5. Figure 5 shows the results of Pedersen *et al.* for Pb-In alloys, and the Thompson and FMMM theoretical curves computed with $\kappa_2(t)$ from Caroli *et al.*[50] and $\kappa_2(t)$ from experimental measurements.[41] Agreement with the Thompson theory is no longer valid and the results, as for the Nb-Ta alloys, are intermediate between the curves representing the two theories. Figure 6 shows our results on Pb-In alloys. The slopes are taken below H_{c2}, where R/R_n has a linear variation with H and, as previously,[13] we find a better agreement with the FMMM theory. We do not present results in the mixed state for the Nb-Mo alloy because the R/R_n curves show a very large rounding near H_{c2} which prevents us from getting meaningful results.

Pedersen *et al.* give a procedure for circumventing the inherent difficulties of measuring the slope of R/R_n near H_{c2}, and their results provide a strong qualitative support for the Thompson theory. Other measurements, using their technique with very-well-homogenized samples, will be useful near T_c. However, in this temperature range, the measurements will always be complicated by

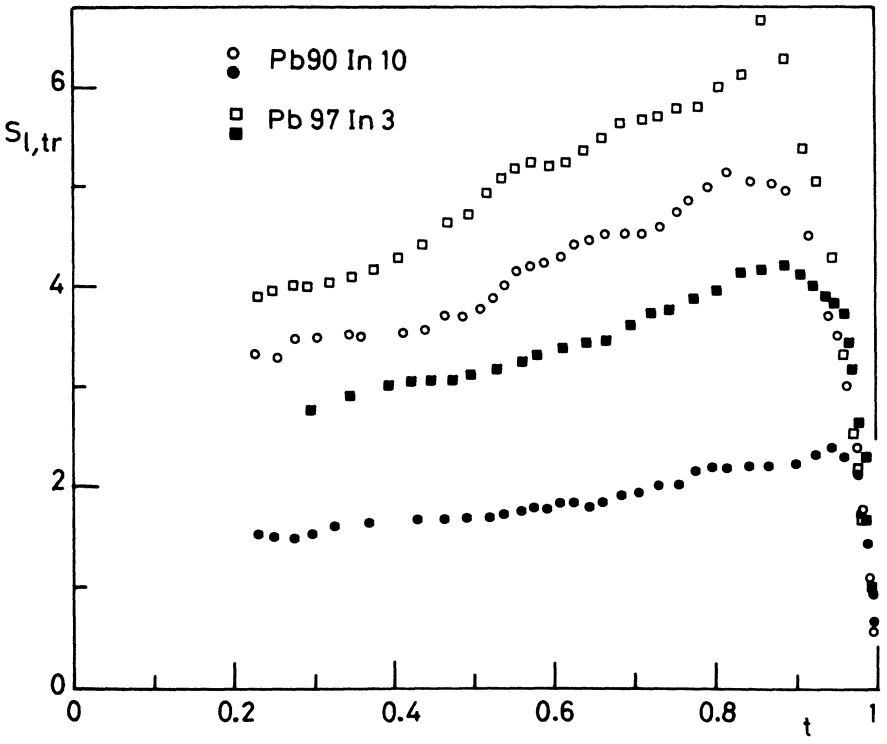

FIG. 7. Temperature variation of the slope of the surface resistence near H_{c3}, $s_{l,tr} = (H/R_n) \times (\partial R/\partial H)\,|_{H=H_{c3}}$ in the longitudinal and transverse orientations for a $Pb_{90}In_{10}$ alloy and a $Pb_{97}In_3$ alloy at 2.4 GHz.

rounding due to thermodynamic fluctuations. For an appropriate interpretation of the results, it will also be necessary to obtain resistivity and magnetization measurements on the same samples in order to determine the true $\kappa_2(t)$ variation.

B. Surface sheath regime

According to Eqs. (14) and (15), it is necessary to have an excellent alignment between H and the surface of the sample. In Ref. 42, R/R_n curves as a function of Θ were shown for different values of H in the transverse orientation. As pointed out in Sec. III, we determine the position of the electromagnet to obtain the minimum value in $R(\Theta)/R_n$ in each experiment.

1. Anisotropy

Typical experimental R/R_n curves in the longitudinal and transverse orientations are given in Fig. 4. It can be seen that R/R_n varies linearly over a large range of the applied magnetic field, and the slopes near H_{c3} can be obtained without difficulty. The variation of R/R_n with H between H_{c2} and H_{c3} becomes more linear as κ increases. For the $Pb_{50}In_{50}$ alloy, when measurements are taken not too close to T_c, R/R_n is a straight line between H_{c2} and H_{c3}. The experimental values of s_{tr} and s_l for $Pb_{90}In_{10}$ and $Pb_{97}In_3$ are shown in Fig. 7, and their ratio A in Fig. 8. In the same figure, the theoretical variation of A with t according to Eq. (18) has been drawn, together with the results of Baixeras and Bodin for a similar specimen.[55] These workers measured A for Pb-In alloys at 600 MHz, the superconductor being the inner conductor of a strip line. They have drawn a regular curve across their experimental s_{tr} and s_l measurements, and the points plotted in Fig. 8 are the ratio of s_{tr}/s_l taken for regularly spaced reduced temperatures on these ideal curves. The uncertainty in their determination of A is indicated for one temperature in Fig. 8. Our measurements show that (not too close to T_c) the anisotropy is almost temperature independent, in good agreement with the Thompson correction of the Maki-Fischer calculation. However we find that, for the $Pb_{90}In_{10}$ and $Pb_{50}In_{50}$ alloys, A is ~0.45, which is 20% lower than the theoretical value of 0.586.

2. Effect of a misalignment on anisotropy

In Fig. 9, we show results for two pieces of the same $Pb_{50}In_{50}$ alloy. Curve (a) is obtained for a sample oxidized during the annealing process, and consequently with a bad surface state after polishing; its anisotropy is strongly temperature dependent. In the same figure, we show the temperature-dependent anisotropy function [Eq. (17)] found by Maki and Fischer[18] [but calculated only in the static range: $\omega \ll \epsilon_0(t)$], together with their experimental results for a $Pb_{91}Bi_9$ alloy which seemed to support their theoretical predictions. Curve (b) is

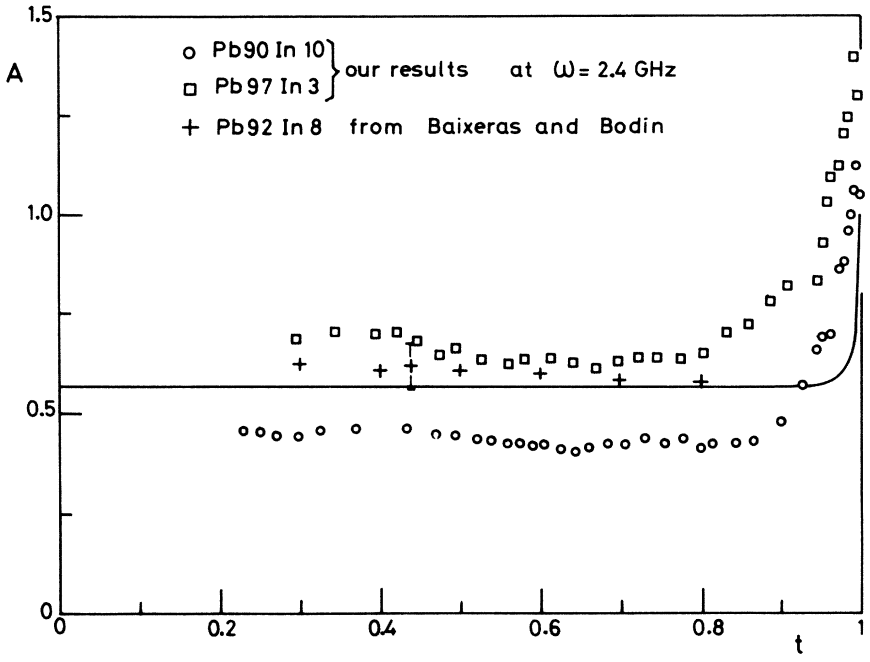

FIG. 8. Anisotropy as a function of $t = T/T_c$ at 2.4 GHz for a $Pb_{90}In_{10}$ alloy and a $Pb_{97}In_3$ alloy. The curve is the theoretical variation of A according to Eq. (18). (+) corresponds to the results obtained by Baixeras and Bodin at 600 MHz.

for a piece of the same $Pb_{50}In_{50}$ alloy, but with a well-polished surface, its anisotropy is almost temperature independent. It can be seen that the values of anisotropy for these two samples are identical for $t > 0.95$. We also measured the anisotropy for the $Nb_{80}Mo_{20}$ alloy. Although this sample may not have been very homogeneous, thus preventing us from obtaining results in the mixed state, the R/R_n curves near H_{c3} were linear enough to get s_{tr} and s_l without ambiguity. We measured R/R_n in the longitudinal ($\Theta = 0$, $\phi = 0$) and transverse ($\Theta = 0$, $\phi = \pi/2$) orientation, and with the magnetic field tilted by 2° from the longitudinal orientation ($\Theta = 2°$, $\phi = 0$). The variations of s_l and s_{tr}, as well as the variation of A with t, are shown in Fig. 10. The anisotropy is much less temperature dependent when $\Theta = 0$ than when $\Theta = 2°$, and, as in Fig. 9, there is no difference in the vicinity of T_c in the two sets of measurements. The results in Figs. 9 and 10 can be explained in the same way. Previously, Monceau and Gilchrist[42] showed that it was unlikely to have H strictly parallel to the sample surface, due to irregularities or undulations of the surface, as well as nonuniformity of H. They developed a

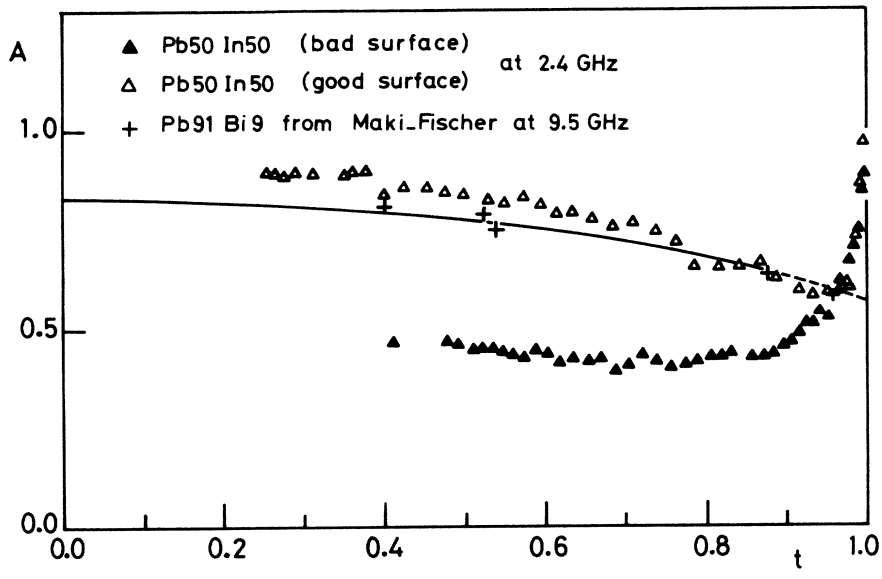

FIG. 9. Anisotropy as a function of t for two pieces of the same $Pb_{50}In_{50}$ alloy, (a) with a bad surface state and (b) with a well-polished surface. The curve is the temperature-dependent theoretical variation of A [Eq. (17)] according to Maki and Fischer and (+) denotes their experimental results at 9.5 GHz for a $Pb_{91}Bi_9$ alloy.

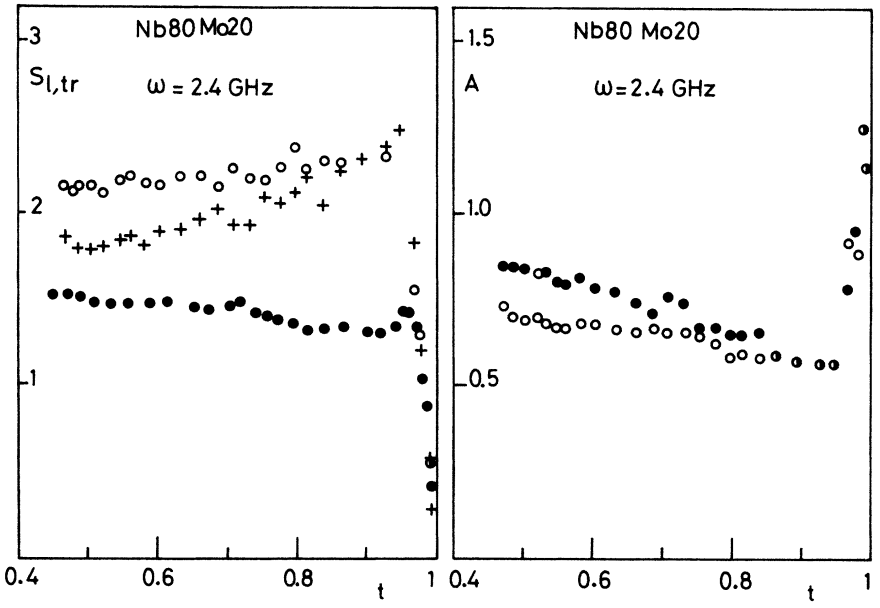

FIG. 10. Right-hand part shows the variation of $s_{l,tr}$ as a function of t for a $Nb_{80}Mo_{20}$ alloy at 2.4 GHz; (0) is s_l with $\theta = 0$ and $\phi = 0$ and (●) s_{tr} with $\theta = 0$, $\phi = \frac{1}{2}\pi$ (+) are the slopes measured when θ is tilted by 2° from the surface (with $\phi = 0$). The left-hand part is the temperature variation of A; (0) corresponds to the ratio s_{tr}/s_l with $s_l(\theta = 0,\ \phi = 0)$ and (●) with $s_l(\theta = 2°,\ \phi = 0)$.

model in which the surface should be decomposed into elements which make different angles with H. If Θ_0 is the average value of Θ between H and a perfectly aligned surface, each surface element makes an angle $\Theta = \Theta_0 + \Psi$ with H; they assumed that Ψ had a Gaussian distribution. The theoretical angular dependence of R/R_n, as calculated from Eqs. (14) and (15) for an ideal surface $[(2\langle\Psi^2\rangle)^{1/2} = 0]$, is much more abrupt than had been experimentally found.[42] The results of Fig. 9 correspond to $\Theta = 0$, but $(2\langle\Psi^2\rangle)^{1/2} \neq 0$ because of important surface irregularities due to a faulty polishing process. The results of Fig. 10 correspond to $\Theta \neq 0$, and ideally to $(2\langle\Psi^2\rangle)^{1/2} = 0$ (but, in a practical sense, as can be seen from the residual temperature dependence of A, $(2\langle\Psi^2\rangle)^{1/2}$ must be not equal to 0 in this alloy, because of the difficulties in getting a good surface state). We see that the theoretical temperature dependence of A [when there is a constant misalignment between H and the surface], calculated by Maki and shown in Fig. 3, is greater than was found experimentally in Figs. 9 and 10. However, there is a good qualitative agreement. In particular, we find that, near T_c, a slight misalignment of H with the surface has no effect on the anisotropy. This is so because, according to Eq. (16), $\tilde{\omega}$ is proportional to $[(1-t)\sin\Theta]^{-1}$, and $\tilde{\omega}$ for a fixed value of Θ becomes $\gg 1$ near T_c. Experimentally, we find that this occurs for $t = 0.95$. Thus, the temperature dependence of A, as found earlier by Maki and Fischer,[18] can be explained either by a constant misalignment of H with the surface, or by a bad surface state of their samples, both faults having the same effect (we, however, must keep in mind that at the frequency of 9.5 GHz the dependence of R/R_n on ω is less drastic than in our experiments).

3. *Behavior of anisotropy near T_c*

In Fig. 11, on an expanded scale, we present the results of the variation of the anisotropy near T_c. Because of the rounding of the R/R_n curves near H_{c3} in the vicinity of T_c we determine the slopes $\partial R/\partial H$ for $R/R_n = 0.90$. The experimental results show that $A = 1$ at $T = T_c$. These are the first anisotropy measurements made in this temperature range, and they give strong support to the theory of fluctuations of the order parameter as an ex-

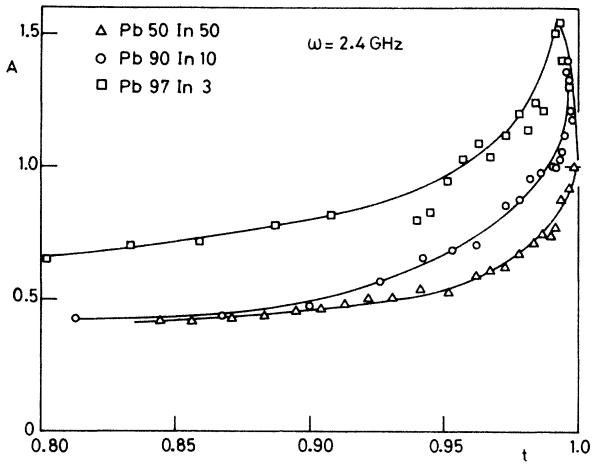

FIG. 11. Anisotropy near T_c at 2.4 GHz. For the $Pb_{90}In_{10}$ and $Pb_{97}In_3$ alloys, the anisotropy is higher than 1 before being equal to 1 at $T = T_c$. The curves are not theoretical, but only to help the eye to follow the variation of A.

planation of this anisotropy. Near T_c, in the transverse orientation, the spatial variation of the order parameter [the relaxation time of which is $\sim \epsilon_0(t)$] cannot follow the exciting field at frequency ω, and the response function is only the static one, as in the longitudinal orientation. The experimental temperature dependence of A near T_c depends strongly on the ratio $\omega/\epsilon_0(t)$ and is less abrupt than the theoretical temperature dependence as shown in Fig. 2. Something similar was found in the study of the dynamical fluctuations near T_c in the mixed state.[14] It has been suggested that, because of the strong coupling behavior of lead-based alloys, $\epsilon_0(t)$ must be replaced by a renormalized $\epsilon_0^*(t)$; with $\epsilon_0^*(t) = 2.2\epsilon_0(t)$, it was possible to reach better agreement between experimental and theoretical results. In Fig. 11, we see that, for the $Pb_{50}In_{50}$ alloy, A has no peak near T_c; the $Pb_{90}In_{10}$ alloy has a small peak; and the $Pb_{97}In_3$ alloy has a higher and broader peak. In Sec. II, it has been pointed out [see Fig. (2)] that A had a peak near T_c when Eq. (7) was satisfied; i.e. when $\xi(t) \gg \mathrm{Re}\delta$ or, similarly, when $\omega/\pi(T_c - T) \gg 2\kappa_2^2$. Experimentally, the $Pb_{97}In_3$ alloy has a peak at $t = 0.993$; for this temperature $\xi = 4600$ Å compared to $\delta = 16\,000$ Å. Moreover, the amplitude of this peak is much higher than its theoretical value. But the agreement with the theoretical predictions is qualitatively good. In particular we find, as stipulated by Eq. (7), that the temperature range where a peak is observed becomes smaller when κ increases.

C. Inclined magnetic field

We now consider the angular dependence of surface impedance when Θ is much larger than the characteristic angle $\Theta_c = \omega/4eDH_{c3}(t)$. In Fig. 12, the normalized slope $s(\Theta)$ as a function of Θ in the transverse orientation is drawn (it was impossible to have large Θ in the longitudinal orientation because of the small perpendicular magnetic field available). First, it is evident that $s(\Theta)$ does not follow Eq. (15). According to Eq. (15), for $\Theta > \Theta_c$, $\tilde{\omega}^2/(1+\tilde{\omega}^2)$ is negligible; $s(\Theta)$ increases slightly due to the Θ dependence of $\mathfrak{a}(H, \Theta)$. Experimentally, we observe a regular decrease in $s(\Theta)$. The difficulty arises from the constant term in Eq. (15). Mathematically it is a consequence of the Hilbert space $(\phi_0, \phi_1)\times(\Psi_0, \Psi_1)$, where ϕ_0, ϕ_1 are the ground-state and the first-excited-state wave functions for the mixed state, and Ψ_0, Ψ_1 are those for the surface sheath, chosen by Maki[30] in order to obtain the ground state and the first excited state in the tilted orientation. But, as pointed out by Maki,[38] there are many other states which have smaller damping constants, and which are very important in the transverse orientation; so it would be necessary to construct more precise wave functions within the space defined by $(\phi_0, \phi_1, \ldots, \phi_n)\times(\Psi_0, \Psi_1)$. Physically, when H is tilted away from the longitudinal orientation the Magnus force on the tilted vortices, $\vec{E}_\omega \times \vec{H}$ is constantly in the surface plane of the sample; but, when H is tilted away from the transverse orientation, $\vec{E}_\omega \times \vec{H}$ has a variable angle $\pi/2 - \Theta$ with the surface, and there is an interaction between the tilted vortices and the surface sheath. It is this interaction which is only approximated by Maki and needs further investigation.[56] Second, we do not find the peak structure in the variation of $s(\Theta)$ that we observed in our measurements on "pseudobulk" samples as defined by $\xi(t) \ll d \ll \delta_0$.[32] These peaks are believed to be some "geometrical resonances" between the tilted vortex lattice and the surface sheath which occurs for specific angles. It has been shown that this peak structure was observed only if the slope $s(\Theta)$ was taken in the subcritical regime very close to $H_{c3}(\Theta)$, and it disappeared if $s(\Theta)$ was measured in the steepest part of R/R_n below H_{c3}. R/R_n for the bulk samples has an almost linear variation between H_{c2} and H_{c3}; this differs from what happens in the case of pseudobulk samples. The slopes in Fig. 12 were taken over a large range of the magnetic field and, so, it is not surprising that $s(\Theta)$ has a monotonic and regularly decreasing variation as a function of Θ.

V. CONCLUDING REMARKS

We have studied the dynamical properties of type-II superconductors for the principal orientations between the static magnetic field H, the microwave field E_ω, and the surface of the sample.

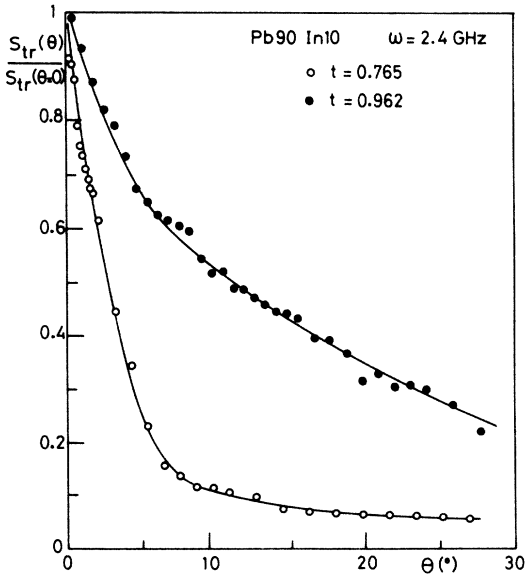

FIG. 12. Angular dependence of the slope of the surface resistance near $H_{c_3}(\Theta)$ normalized for $\Theta = 0$ as a function of Θ.

The results can be successfully interpreted by the oscillations or fluctuations of the order parameter as first suggested by Caroli and Maki,[7] but with the Thompson corrections.[10,20] We have noted that, in the mixed state, it is very difficult to obtain measurements close enough to H_{c2} to get the "anomalous term" in the conductivity. This anomalous term comes from the static limit of the imaginary part of the response function. In the surface sheath regime, our results show that the anisotropy is temperature independent, as calculated by Thompson.[20] This anisotropy is the ratio between the real part of the response function in the transverse and longitudinal orientation, and includes only regular terms. Walton *et al.*[25] have recently tried to explain this anisotropy in microwave experiments completely outside the scope of the formalism developed above. In the study of the superheated state, Kramer[57] found some Ginsburg-Landau solutions with zero values of the order parameter along the surface. Walton and Rosenblum[26] postulated the existence of these vortices or "nascent vortices," below H_{c2}, in order to explain the hysteresis observed in their microwave measurements. Rothwarf *et al.*[22] calculated the surface resistance in the longitudinal orientation, above H_{c2}, with a two-layer model with the surface sheath on the top of the normal bulk. Below H_{c2}, as seen in Fig. 4, the surface resistance decreases very rapidly because the mixed state is not absorbing, the microwave currents being parallel to the vortices. Walton *et al.*[25] claimed that the high surface-resistance value in the transverse orientation was not due to the resistivity of the mixed state in this orientation but to the conductivity of the surface sheath itself, and that the model, below H_{c2}, must be a three-layer one: the nascent vortices layer, with a conductivity equal to the one in the mixed state; the surface sheath; and the bulk in the mixed state. We should like to make some comments about this interpretation. First, we have never observed intrinsic hysteresis in the transverse orientation as reported by Cardona *et al.*[58] or Walton and Rosenblum.[26] The phenomenological model of Walton *et al.*[25] is applicable to all magnetic fields between H_{c1} and H_{c3}, whereas the Thompson[20] theory is restricted to the Ginsburg-Landau range; i.e., $H_{c3}(t) - H \ll H_{c3}(0)$. But, for high κ, the R/R_n curves are linear between H_{c2} and H_{c3} and we think that the Thompson theoretical expressions are valid between these two fields. Walton *et al.* estimate that, on the top of the surface sheath in which the order parameter is always in the ground state, a layer similar to the mixed state exists; this layer would be much more absorbing when the microwave current is perpendicular to the vortices than when it is parallel. The alternative explanation is that the order parameter in the surface sheath is in the ground state in the longitudinal orientation only, whereas in the transverse orientation it is in the excited state; our results in agreement with theory[20] are a strong support to this explanation. Our experimental results showing the disappearance of the anisotropy near T_c are also a confirmation of the order-parameter fluctuations. Near T_c, the oscillations of the order parameter with their relaxation frequency $\epsilon_0(t)$ cannot follow the exciting field at frequency ω and, consequently they are not excited; the anisotropy there is equal to 1. But we have also considered the existence of zero-order-parameter regions in the surface sheath; this is the Kulik or inclined vortices state, due to a misalignment between H and the surface of the sample. This structure, however, has the effect of reducing the anisotropy. The dynamical properties of these inclined vortices have been studied. The surface resistance is strongly dependent on the parameter $\tilde{\omega} = \omega/3.4\epsilon_0 \sin\Theta$, and it is only when $\tilde{\omega} \gg 1$ that it equals the result obtained when H is strictly parallel to the surface. We have shown experimentally that, at low temperatures, a slight misalignment has a drastic effect on the anisotropy of the surface resistance but, near T_c, when ϵ_0 is small, we find the same result as in the parallel orientation. Finally, in the study of microwave surface impedance, one of the remaining theoretical problems is to obtain expressions valid for large Θ when H is tilted away from the surface.

ACKNOWLEDGMENTS

We should like to thank C. Caroli, G. Fischer, J. le G. Gilchrist, K. Maki, B. Rosenblum, D. Saint-James, and R. S. Thompson for fruitful discussions on the problems treated here. We are grateful to K. Maki for illuminating correspondence, to B. Rosenblum and B. L. Walton for their report of work prior to publication, to J. le G. Gilchrist for his constant encouragement, and to J. Bret for his experimental assistance. We also thank O. Samson for the reading of the manuscript.

APPENDIX

The Q'_{stat} response function is given by Eq. (29) of Caroli and Maki[7]

$$Q'_{stat} = \frac{\sigma_n |\Delta|^2}{2\pi T} \left\{ \Psi^{(1)}\left(\frac{1}{2} - \frac{i\omega}{2\pi T} + \rho_0\right) + 2\pi T \left(\frac{1}{-i\omega} + \frac{1}{-i\omega + \epsilon_0}\right) \left[\Psi\left(\frac{1}{2} - \frac{i\omega}{2\pi T} + \rho_0\right) - \Psi\left(\tfrac{1}{2} + \rho_0\right)\right] \right\} .$$

If $\omega \ll \pi T_c$, we can develop the digamma functions and

$$Q'_{\rm stat}=\frac{\sigma_n|\Delta|^2}{\pi T}\Psi^{(1)}(\tfrac{1}{2}+\rho_0)\left[1+\frac{1}{2}\,\frac{-i\omega}{-i\omega+\epsilon_0}-\frac{i\omega}{8\pi T}\left(3+\frac{-i\omega}{-i\omega+\epsilon_0}\,\frac{\Psi^{(2)}(\frac{1}{2}+\rho_0)}{\Psi^{(1)}(\frac{1}{2}+\rho_0)}\right)\right]\ . \tag{A1}$$

Q'_T is given by Eq. (10) of Ref. 10 as corrected in footnote 5 of Ref. 20:

$$Q'_T=-\sigma_n|\Delta|^2\sum_n x_n\left\{\frac{1}{4\pi T}\left[\frac{1}{\epsilon_{n0}-i\omega}\Psi^{(1)}(\tfrac{1}{2}+\rho_0)+\frac{1}{\epsilon_{n0}+i\omega}\Psi^{(1)}\left(\frac{1}{2}-\frac{i\omega}{2\pi T}+\rho_0\right)\right]\right.$$
$$\left.+\frac{4(\epsilon_{n0})^2}{(\epsilon_{n0}^2+\omega^2)^2}\left[\Psi(\tfrac{1}{2}+\rho_0)-\Psi\left(\frac{1}{2}-\frac{i\omega}{4\pi T}+\rho_i+\rho_0\right)\right]+\frac{1}{i\omega}\,\frac{\epsilon_{n0}}{(\epsilon_{n0}+i\omega)^2}\left[\Psi(\tfrac{1}{2}+\rho_0)-\Psi\left(\frac{1}{2}-\frac{i\omega}{2\pi T}+\rho_0\right)\right]\right\}\ ,$$

$\rho_i=\epsilon_{n0}/4\pi T$.

$Q'_{\rm CM}$ is given by Eq. (31) of Caroli-Maki[7]

$$Q'_{\rm CM}=-\sigma_n|\Delta|^2\sum_n x_n\left\{\frac{4(\epsilon_{n0})^2}{(\omega^2+\epsilon_{n0}^2)^2}\left[\Psi(\tfrac{1}{2}+\rho_0)-\Psi\left(\frac{1}{2}-\frac{i\omega}{4\pi T}+\rho_i+\rho_0\right)\right]\right.$$
$$\left.+\frac{4\epsilon_{n0}}{\omega^2+\epsilon_{n0}^2}\,\frac{1}{\epsilon_{n0}+i\omega}\left[\Psi(\tfrac{1}{2}+\rho_0)-\Psi\left(\frac{1}{2}-\frac{i\omega}{2\pi T}+\rho_0\right)\right]+\frac{1}{[\epsilon_{n0}+i\omega]^2}\,\frac{[\Psi(\frac{1}{2}+\rho_0)-\Psi(\frac{1}{2}-i\omega/2\pi T+\rho_0)]^2}{[\Psi(\frac{1}{2}-i\omega/4\pi T+\rho_i+\rho_0)-\Psi(\frac{1}{2}+\rho_0)]}\right\}\ ,$$

$Q'_{\rm fluct}=Q'_T+Q'_{\rm CM}$.

There are important cancellations between Q'_T and $Q'_{\rm CM}$

$$Q'_{\rm fluct}=-\sigma_n|\Delta|^2\sum_n x_n\left\{\frac{1}{4\pi T}\left[\frac{1}{\epsilon_{n0}-i\omega}\Psi^{(1)}(\tfrac{1}{2}+\rho_0)+\frac{1}{\epsilon_{n0}+i\omega}\Psi^{(1)}\left(\frac{1}{2}-\frac{i\omega}{2\pi T}+\rho_0\right)\right]\right.$$
$$+\left(\frac{1}{i\omega}\,\frac{\epsilon_{n0}}{(\epsilon_{n0}+i\omega)^2}+\frac{1}{(\epsilon_{n0}+i\omega)}\,\frac{4\epsilon_{n0}}{(\omega^2+\epsilon_{n0})^2}\right)\left[\Psi(\tfrac{1}{2}+\rho_0)-\Psi\left(\frac{1}{2}-\frac{i\omega}{2\pi T}+\rho_0\right)\right]$$
$$\left.+\frac{1}{(\epsilon_{n0}+i\omega)^2}\,\frac{[\Psi(\frac{1}{2}+\rho_0)-\Psi(\frac{1}{2}-i\omega/2\pi T+\rho_0)]^2}{[\Psi(\frac{1}{2}-i\omega/4\pi T+\rho_i+\rho_0)-\Psi(\frac{1}{2}+\rho_0)]}\right\}\ ;$$

this is Eq. (75) of Ref. (30). If $\omega\ll\pi T_c$ we can expand the above expression in powers of ω/T_c and we get the low-frequency expression of $Q'_{\rm fluct}$:

$$Q'_{\rm fluct}=-\frac{\sigma_n|\Delta|^2}{\pi T}\,\Psi^{(1)}(\tfrac{1}{2}+\rho_0)$$
$$\times\sum_n x_n\left[\frac{4}{\epsilon_{n0}-i\omega}\left(1-\frac{i\omega}{4\pi T}\,\frac{\Psi^{(2)}(\frac{1}{2}+\rho_0)}{\Psi^{(1)}(\frac{1}{2}+\rho_0)}\right)\right]\ . \tag{A2}$$

The average value of the order parameter is defined in the mixed state by the expression

$$-4eM=(\sigma_n/\pi T)\,\Psi^{(1)}(\tfrac{1}{2}+\rho_0)\,\langle|\Delta|^2\rangle$$
$$=\frac{e}{\pi}\,\frac{H_{c_2}(t)-H}{1.16[2\kappa_2^2(t)-1]+n}\ . \tag{A3}$$

In the surface sheath Maki[37] has calculated the average value of $|\Delta|^2$ which can be written

$$\frac{\sigma_n}{\pi T}\,\Psi^{(1)}(\tfrac{1}{2}+\rho_0)\,\frac{1}{\xi(t)}\int_0^\infty|\Delta(z)|^2\,dz$$
$$=(\tfrac{1}{2}\pi)^{1/2}\,\frac{0.59e}{\pi}\,\frac{H_{c_3}(t)-H}{2\kappa_2^2(t)-0.328}\ . \tag{A4}$$

---

*This paper is a part of a docteur-ingenieur thesis of Y. Brunet submitted to the University of Grenoble (1972).

†Laboratoire associé au Centre National de la Recherche Scientifique.

[1]For a review of transport properties in type-II superconductors, see Y. B. Kim, in *Proceedings of the Twelfth International Conference on Low Temperature Physics, Kyoto, Japan*, edited by E. Kanda (Academic Press of Japan, Tokyo, 1971), p. 231.

[2]J. Bardeen and M. J. Stephen, Phys. Rev. 140, A1197 (1965).

[3]B. Rosenblum and M. Cardona, Phys. Rev. Lett. 12, 657 (1964).

[4]P. Nozières and W. F. Vinen, Philos. Mag. 14, 667 (1966).

[5]Y. B. Kim, C. F. Hempstead, and A. R. Strnad, Phys. Rev. 139, A1163 (1965).

[6]A. Schmid, Phys. Kondens. Mater. 5, 302 (1966).
[7]C. Caroli and K. Maki, Phys. Rev. 159, 306 (1967).
[8]C. Caroli and K. Maki, Phys. Rev. 164, 591 (1967).
[9]H. Takayama and H. Ebisawa, Prog. Theor. Phys. 44, 1450 (1970).
[10]R. S. Thompson, Phys. Rev. B 1, 327 (1970).
[11]L. P. Gor'kov and G. M. Eliashberg, Zh. Eksp. Teor. Fiz. 54, 612 (1968) [Sov. Phys.-JETP 27, 328 (1968)].
[12]For a review of time-dependent Ginsburg-Landau equations, see M. Cyrot, Rep. Prog. Phys. 36, 103 (1973).
[13]G. Fischer, R. D. McConnell, P. Monceau, and K. Maki, Phys. Rev. B 1, 2134 (1970).
[14]G. Fischer, R. D. McConnell, P. Monceau, and K. Maki, Phys. Rev. B 2, 2817 (1970).
[15]D. Saint-James and P. G. de Gennes, Phys. Lett. 7, 306 (1963).
[16]K. Maki, Phys. Rev. 141, 331 (1966).
[17]G. Fischer and K. Maki, Phys. Rev. 176, 581 (1968).
[18]K. Maki and G. Fischer, Phys. Rev. 184, 472 (1969).
[19]The anisotropy of the surface impedance in the surface sheath regime was first observed by M. Cardona and B. Rosenblum, Phys. Lett. 8, 308 (1964).
[20]R. S. Thompson, Phys. Rev. B 3, 1617 (1971).
[21]B. Rosenblum, *Proceedings of the Eleventh International Conference on Low Temperature Physics, St. Andrews, Scotland*, 1968, edited by J. S. Allen, D. M. Finlayson, and D. M. McCan (University of St. Andrews, St. Andrews, Scotland, 1969).
[22]A. Rothwarf, J. I. Gittleman, and B. Rosenblum, Phys. Rev. 155, 370 (1967).
[23]H. J. Fink and R. D. Kessinger, Phys. Rev. 140, A1937 (1965).
[24]C. J. Gorter and H. B. G. Casimir, Z. Phys. 35, 963 (1934).
[25]B. L. Walton, B. Rosenblum, and F. Bridges, Phys. Lett. A 43, 263 (1973).
[26]B. L. Walton and B. Rosenblum, in *Proceedings of the Thirteenth International Conference on Low Temperature Physics, Boulder, Colorado*, edited by R. H. Kropschot and K. D. Timmerhaus (University of Colorado Press, Boulder, Colo., 1973).
[27]P. Monceau, thesis University of Grenoble, 1970), (unpublished).
[28]I. O. Kulik, Zh. Eksp. Teor. Fiz. 55, 889 (1968) [Sov. Phys.-JETP 28, 461 (1969)].
[29]K. Maki, J. Low Temp. Phys. 3, 545 (1970).
[30]K. Maki, in *Quantum Fluid (Tokyo Summer Institute for Theoretical and Experimental Physics)*, edited by R. Kubo and F. Takano (Syokabo, Tokyo, 1970).
[31]A preliminary report of the results of this present work is published in Ref. 26, p. 160.
[32]P. Monceau, D. Saint-James, and G. Waysand, in Ref. 26, p. 152; P. Monceau, D. Saint-James, and G. Waysand (unpublished).
[33]H. J. Fink, Phys. Rev. 177, 732 (1969).
[34]D. Saint-James, Phys. Lett. 16, 218 (1965).
[35]R. J. Pedersen, Y. B. Kim, and R. S. Thompson, Phys. Rev. B 7, 982 (1973).
[36]H. Takayama and K. Maki, J. Low Temp. Phys. 12, 195 (1973).
[37]K. Maki, in *Superconductivity*, edited by R. D. Parks (Dekker, New York, 1969), Chap. 18.
[38]K. Maki (private communication).
[39]A. B. Pippard, Proc. R. Soc. A 191, 370 (1947).
[40]J. R. Waldram, Adv. Phys. 13, 1 (1964).
[41]J. le G. Gilchrist and P. Monceau, J. Phys. C 3, 1399 (1970).
[42]P. Monceau and J. le G. Gilchrist, J. Low Temp. Phys. 5, 363 (1971).
[43]J. Mazuer, Y. Brunet, J. Gilchrist, P. Monceau, and J. Odin, Rev. Phys. Appl. 6, 377 (1971).
[44]H. K. Worner and H. W. Worner, J. Inst. Met. 66, 45 (1940).
[45]J. G. Adler, J. E. Jackson, and T. A. Will, Phys. Lett. A 24, 407 (1967).
[46]J. Bardeen, L. N. Cooper, and J. R. Schrieffer, Phys. Rev. 108, 1175 (1957).
[47]R. A. French and J. Lowell, Phys. Rev. 173, 504 (1968).
[48]B. B. Goodman and G. Kuhn, J. Phys. (Paris) 29, 240 (1968).
[49]D. K. Finnemore, T. F. Stromberg, and C. A. Swenson, Phys. Rev. 149, 231 (1966).
[50]C. Caroli, M. Cyrot, and P. G. de Gennes, Solid State Commun. 4, 17 (1966).
[51]G. Eilenberger, Phys. Rev. 153, 584 (1967).
[52]K. D. Usadel, Phys. Rev. B 2, 135 (1970).
[53]A. Ikushima and T. Mizusaki, J. Phys. Chem. Solids 30, 873 (1969).
[54]D. E. Farrell, B. S. Chandresekhar, and H. V. Culbert, Phys. Rev. 177, 694 (1969).
[55]J. Baixeras and C. Bodin, Rev. Phys. (Paris) 33, 407 (1972).
[56]P. Monceau and G. Waysand, Rev. Phys. Appl. 8, 413 (1973).
[57]L. Kramer, Z. Phys. B 259, 333 (1973).
[58]M. Cardona, J. Gittleman, and B. Rosenblum, Phys. Lett. 17, 95 (1965).